MECHANIKA TEORETYCZNA
I STOSOWANA
Journal of Theoretical
and Applied Mechanics
3, 33, 1995

INFLUENCE OF INDUCED VELOCITY MODELLING ON HELICOPTER STABILITY

PAWEŁ MAZUREK

Aviation Institute, Warsaw

JANUSZ NARKIEWICZ

Institute of Aeronautics and Applied Mechanics
Warsaw University of Technology, Warsaw

An influence of modelling of main rotor induced velocity distribution on helicopter stability is investigated for various flight conditions: hover, vertical and forward flight with and without the ground effect.
Closed formulae describing rotor inflow models are reviewed and their applicability to stability analysis is evaluated. Selected inflow models are utilised for calculation of parameters of steady flight, linearized equations of helicopter motion and eigenvalues and eigenvectors of the state matrix.
Investigation of stability of a helicopter in steady flight reveals that the differences between the results obtained using different formulae based on the Glauert method i.e., harmonic for azimuth and linear along the blade are negligible.
Other induced velocity models, like the Mangler-Squire and dynamic inflow, do not change the character of helicopter motion but they influence quantitatively the results of stability investigation.

Notation

a	–	lift curve slope for a blade aerofoil, $dC_L/d\alpha$
A	–	rotor disc area, $A = \pi R_w^2$
b	–	number of rotor blades
$c(r)$	–	blade chord
C_{amx}	–	coefficient of rotor aerodynamic roll moment, $C_{amx} = 2M_x/(\rho A R_w V_T)$

C_{amy}	–	coefficient of rotor aerodynamic pitch moment, $C_{amy} = 2M_y/(\rho A R_w V_T)$
C_T	–	thrust coefficient, $C_T = 2T/(\rho A V_T)$
M_x, M_y	–	rotor aerodynamic roll and pitch moments
P, Q, R	–	components of helicopter angular velocity
r	–	distance of blade section from rotor axis
R_w	–	rotor radius
$\boldsymbol{S}$	–	vector of steady flight parameters, $\boldsymbol{S} = [\theta, \phi, \Theta_0, \Theta_1, \Theta_2, \Theta_{so}]$
t_4	–	integral of rotor blade taper
T	–	rotor thrust
U, V, W	–	components of helicopter velocity
V_T	–	rotor tip speed velocity, $V_T = \Omega R_w$
$\boldsymbol{X}$	–	helicopter flight state vector, $\boldsymbol{X} = [U, V, W, P, Q, R]$
Z	–	distance from the rotor to the ground
α_w	–	rotor disc angle of incidence
β	–	rotor blade flapping angle
Θ	–	angle of rotor blade pitch control
Θ_{so}	–	angle of tail rotor collective pitch control
θ	–	helicopter pitch angle
χ	–	wake skew angle, $\chi = \lambda/\mu$
λ_c	–	coefficient of vertical flight velocity, $\lambda_c = W/V_T$
λ_i	–	induced velocity coefficient, $\lambda_i = v_i/V_T$
λ_{ih}	–	induced velocity coefficient in hover
μ	–	helicopter advance ratio coefficient
ρ	–	air density
σ_R	–	coefficient of rotor solidity, $\sigma_R = bc(0)/(\pi R_w)$
ϕ	–	helicopter roll angle
ψ	–	azimuth of the main rotor
Ω	–	angular velocity of the main rotor.

Index g relates to the ground effect.

1. Introduction

In aircraft design and modification it is important to have a chance for predicting its performance, flying qualities and stability using analytical tools supported by computer facilities. Behaviour of prospective aircraft should be investigated well in advance both because of safety requirements and law regulations [1]. For instance, tests in flight should be preceded by evaluations of aircraft airworthiness. Methods used in practice for such an analysis should be reliable and as efficient as possible in terms of computation time. This is a good reason for developing and applying rather simple models to analysis of this type.

A helicopter model is usually composed of main and tail rotor, fuselage and stabilisers. These elements are subjected to inertia, aerodynamic and stiffness loads, which depend on displacements, velocities and accelerations of the whole aircraft and its components relative to each other.

A main rotor is the most important part in these analysis because it acts as a device for producing lift, propulsive force and control moments. Aerodynamic loads form a crucial part of a rotor model, because of complex flow environment, which results from rotor blade motion relative to the fuselage and to the ground, proximity of the rotor wake to blades and periodic excitations in forward flight.

A flow velocity around the rotor blade is a sum of velocities coming from:

- Helicopter flight
- Rotation about shaft axis with angular velocity
- Motion of blades in a rotating frame of reference which comes from pitch control, rotations in hinges and/or blade deflections
- Variations of air velocity due to gusts or turbulence.

The shape of rotor wake depends on the flight conditions (velocity and ground proximity), number of blades, blade pitch angle, rotor disk loading, distance from the rotor to other parts of a helicopter. Methods of Computational Fluid Dynamic which would deal successfully with a complicated unsteady wake shape of a helicopter rotor are still in a phase of development and up till now they cannot be treated as an efficient tool in solving practical problems of rotor aerodynamic. So, in routine calculations, there is still a place for various simplified methods.

Simplifying assumptions commonly used in modelling of the rotor flow concern analysis of the wake shape separate from calculation of load, which is

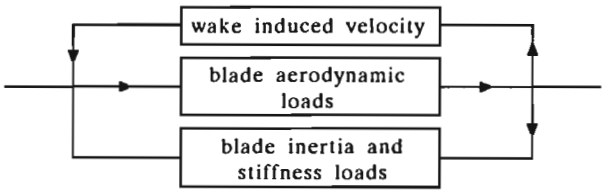

Fig. 1. Modelling of rotor aerodynamic loads

illustrated in Fig.1. In this case the influence of rotor wake on the flow around the blades is modelled as an induced velocity, which changes the distribution of angle of attack along the blade. The aerodynamic load are then calculated from other model, for instance using aerodynamic coefficients obtained from airfoil tests in wind tunnel or the unsteady airfoil theory (cf Narkiewicz and Syryczyński (1992)).

The induced velocity distribution over the rotor disc can be computed with various scope of complexity. The review of methods used for calculation of the induced velocity is done for instance, by Chen (1989).

The objective of this study is to investigate the influence of induced velocity modelling on stability of a single rotor helicopter. Similar research was undertaken by Kowaleczko (1991), but with limited number of models considered.

In the research presented in this paper, the model (cf Łucjanek et al. (1986)) of a single rotor helicopter is utilised with necessary modifications enabling analysis of different inflow models. Stability of helicopter motion is investigated for hover, vertical and forward flight, with and without ground effects.

2. Review of induced velocity models

There are common assumptions accepted in simplified models of induced velocity. Usually fluid is treated as inviscid and incompressible. The flow can be considered as steady or unsteady, with continuous variation of parameters along the stream lines. A rotor thrust is assumed to result from imposing some mass of air "down" through a rotor disk. Due to air viscosity, the rotor blades "drag" some part of surrounding air also into motion in the plane of blades rotation and cause a swirl of a rotor stream. This component of velocity is

usually neglected in simplified models due to its small value. Only about 2% of the induced power is consumed due to this motion.

In a majority of applications, only the component of induced velocity perpendicular to the rotor disk is taken into account and the distribution of this velocity over the rotor disk is approximated by simple analytical functions. Along the blade, this distribution is usually constant or linear and along the azimuth it is usually expressed as a Fourier series of azimuth angle.

In each particular model there are also specific assumptions which reduce the range of its application.

In the sequel, induced velocity models are considered for hover, vertical (climbing and descending) and forward flight (slow, moderate and fast) with and without ground effect.

In a vertical flight an induced velocity depends mainly on the relation between nondimensional vertical flight velocity λ_c and a disk loading expressed as the rotor induced velocity in hover λ_{ih}.

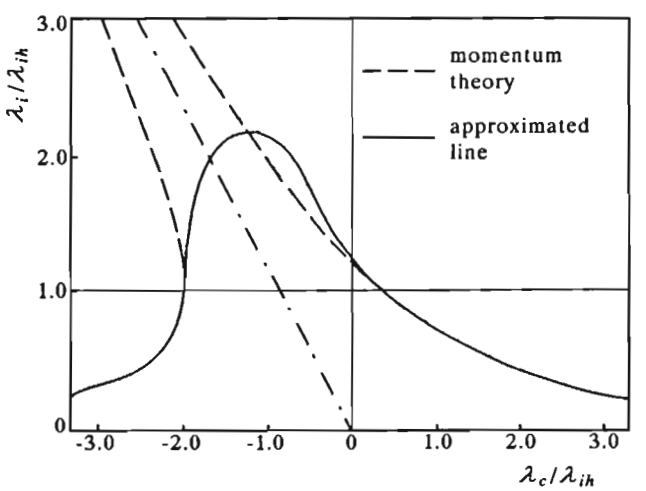

Fig. 2. Mean induced velocity in vertical flight

Different flight conditions are classified in Table 1 and the values of mean induced velocity in axial flight are given in Fig.2.

Table 1

	λ_c	$\lambda_c + \lambda_i$	$\lambda_c + 2\lambda_i$	flight state
1	+	+	+	climb
2	0	+	+	hover
3	−	+	+	vortex ring state
4	−	0	+	ideal autorotation
5	−	−	+	turbulent wake
6	−	−	0	turbulent wake limit
7	−	−	−	windmill state

In vertical climb and in hover, the momentum theory is commonly used for evaluating the average value of induced velocity. In a vortex ring state, the flow through the rotor is disturbed and highly unsteady, so no simple theory is available and approximations of empirical data are used to evaluate the mean value of induced velocity. "Ideal autorotation" means that under these flight conditions energy can be transferred from the stream to the rotor, but due to energy consumption by other than main rotor devices, autorotation of the real helicopter occurs at a higher descending velocity. In a state of turbulent wake the flow through rotor disk is similar the flow around a flat plate. In a windmill state the flow again is still and continuous; momentum theory can be applied.

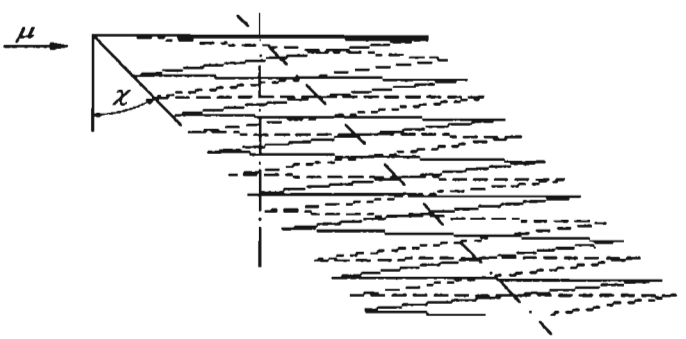

Fig. 3. Rotor wake pattern in forward flight

In helicopter forward flight a flow through rotor disc is skewed. Main parameters in this case are: the nondimensional flight velocity μ and the wake skew angle χ (Fig.3). The measure of wake skew angle χ increases with increase of a flight velocity, so the influence of the wake on rotor blades diminishes with μ.

For $0 < \mu < 0.1$ the wake stays in a proximity to rotor disk. Interference

of wakes produced by different blades and interaction of the rotor wake with the fuselage take place. The rotor stream is disturbed and unsteady.

For $0.1 < \mu < 0.3$ the flow through rotor disk is stable. Simplified methods for calculating the induced velocity can produce reliable results.

For $\mu > 0.3$ the areas of stall on the retreating side and the regions of subsonic flow on the advancing side of rotor disc can appear. These areas contribute to rotor loads and should be accounted for in the stability analysis.

The influence of a ground on distribution of the induced velocity depends on the elevation Z of the rotor over the ground surface and on the magnitude of forward flight velocity μ. The "ground effect" appears as an increase in rotor thrust for a given power and can be taken into account as correction of induced velocity distribution.

The qualitative description of the flow over the helicopter rotor under various flight conditions given above helps in assessment of the applicability and restrictions imposed on different models. The models of induced velocity analysed in this study are collected in Table 2 for the axial flow and in Table 3 for the forward flight. In Table 4 the way of accounting for the ground effect is given.

Description of these models is presented below. First, the models which can be applied to both vertical and forward flight cases are presented. Next, the model valid only for vertical or forward flight is considered and the influence of side velocity and ground effect is analysed.

2.1. General methods

Two models; i.e., Mangle-Squire (MS) and dynamic inflow (DI) are applicable to the helicopter to both vertical and forward flights.

In the model of Mangler-Squire (cf Mangler and Squire (1950); Bramwell (1976)) an induced velocity is expressed as the sum of Fourier series

$$\lambda_i = 4\lambda_{io}\Big[\frac{1}{2}c_0 - \sum_{n=1}^{\infty} c_n(x, \alpha_w)\cos(n\psi)\Big] \tag{2.1}$$

with the coefficients for:

– constant part (zero harmonic)

$$c_0 = \frac{15\mu_0(1-\mu_0)}{8} \tag{2.2}$$

where

$$\mu_0 = \sqrt{1-x^2} \qquad x = \frac{r}{R_w}$$

– nth harmonic

$$c_n = \sqrt{(-1)^{n-2}}\frac{15}{8}\Big[\frac{(x+n)(9x^2+n^2-6)}{(n^2-1)(n^2-9)} + 3x(n^2-9)\Big]\sqrt{(1-x^2)^n(1-\sin^2\alpha_w)^n} \qquad \text{for } n \geq 2 \tag{2.3}$$

$$c_n = 0 \qquad \text{for } n \geq 5$$

The value of λ_{io} is computed from the momentum theory given below (Eqs (2.12) and (2.14)).

In hover and vertical flight the coefficients different from c_0 are equal zero since $\alpha_w = 0$, and

$$\lambda_i = 4c_0\lambda_{io} \tag{2.4}$$

In this study, due to limitations inherent to computer program, only the first harmonic of induced velocity is included into the helicopter stability analysis.

Dynamic inflow model (cf Peters and HaQuang (1988)) accounts for a time delay in variation of induced velocity relative to variation in helicopter motion. In a dynamic inflow model, induced velocity is calculated as

$$\lambda_i = \lambda_{io} + \lambda_{di} \tag{2.5}$$

where

λ_{io} – constant part of induced velocity, calculated usually from the Glauert theory, Eqs (2.12) and (2.14)

λ_{di} – disturbance from dynamic inflow model.

The dynamic inflow disturbance λ_{di} is calculated as

$$\lambda_{di} = \lambda_{i1} + \lambda_{i2}\cos\psi + \lambda_{i3}\sin\psi \tag{2.6}$$

The coefficients λ_{ii} form a solution to a system of differential equation

$$\mathbf{M}\dot{\lambda} + \mathbf{L}^{-1}\lambda = \mathbf{C}_{Fa} \tag{2.7}$$

where the matrices $\mathbf{M}$ and $\mathbf{L}$ are calculated as

$$\mathbf{M} = \begin{bmatrix} \frac{128}{75\pi} & 0 & 0 \\ 0 & \frac{16}{45\pi} & 0 \\ 0 & 0 & \frac{16}{45\pi} \end{bmatrix} \tag{2.8}$$

$$\mathbf{L} = \begin{bmatrix} \frac{1}{2} & 0 & -\frac{15\pi}{64}\sqrt{\frac{1-\sin\alpha_v}{1+\sin\alpha_v}} \\ 0 & \frac{4}{1+\sin\alpha_v} & 0 \\ \frac{15\pi}{64}\sqrt{\frac{1-\sin\alpha_v}{1+\sin\alpha_v}} & 0 & \frac{4}{1+\sin\alpha_v} \end{bmatrix} \begin{bmatrix} \lambda_T & 0 & 0 \\ 0 & \lambda_v & 0 \\ 0 & 0 & \lambda_v \end{bmatrix} \tag{2.9}$$

where

$$\lambda_v = \frac{\mu^2 + (\lambda_m + \lambda_c)(2\lambda_m + \lambda_c)}{\lambda_{iT}} \qquad \lambda_T = \sqrt{(\lambda_m + \lambda_c)^2 + \mu^2} \tag{2.10}$$

$$\alpha_v = \tan^{-1}\frac{|\lambda_m + \lambda_c|}{\mu} \qquad \lambda_m = \frac{1}{2}\begin{bmatrix} 1 \\ 0 \\ 0 \end{bmatrix} \mathbf{L}^{-1} \begin{bmatrix} \lambda_{i1} \\ \lambda_{i2} \\ \lambda_{i3} \end{bmatrix} \tag{2.11}$$

2.2. Axial flow

Despite the general models given above, the group of models applicable to axial flow through rotor contain additionally two methods, given in Table 2.

Table 2

mod. symb.	model formulae	refer.
V1	$\lambda_i = -\frac{\lambda_c}{2} - \left[\left(\frac{\lambda_c}{2}\right)^2 - \lambda_{ih}^2\right]^{0.5}$ $\frac{\lambda_c}{\lambda_{ih}} < -2$ or $\frac{\lambda_c}{\lambda_{ih}} \geq -\frac{1}{2}$	[13]
	$\lambda_i = k\lambda_c\left[0.373\left(\frac{\lambda_c}{\lambda_{ih}}\right)^2 - 1.991\right]$	[8]
V2	$\lambda_i = \left(\frac{\lambda_c}{2} + \frac{bca}{16\pi R_w}\right)\left\{-1 + \left[1 + \frac{2\left(\frac{\Theta r}{R_w} - \lambda_c\right)}{\frac{4\pi\lambda_c R_w^2}{bca} + \lambda_c + \frac{bca}{16\pi R_w}}\right]^{0.5}\right\}$	[7]
MS	$\lambda_i = 4c_0\lambda_{io}$	[11,2]
DN	$\dot{\lambda}_i + (\mathbf{LM})^{-1}\lambda_i = \mathbf{M}^{-1}\mathbf{C}_{Fa}$	[14]

In the model (V1) of Payne (1959) and Johnson (1980) a constant distribution of induced velocity over the rotor disk is assumed. The value of induced velocity in hover is calculated from the momentum theory as

$$\lambda_{ih} = \frac{\sqrt{C_T}}{2} \tag{2.12}$$

which is valid for helicopter climb, hover and descend at a moderate velocity. For descending at small velocities the approximation of empirical data (Fig.4) is applied.

In the model (V2) of Gessow and Meyers (1985) the induced velocity is calculated by the strip theory and it is a non-linear function of the distance from the rotor centre.

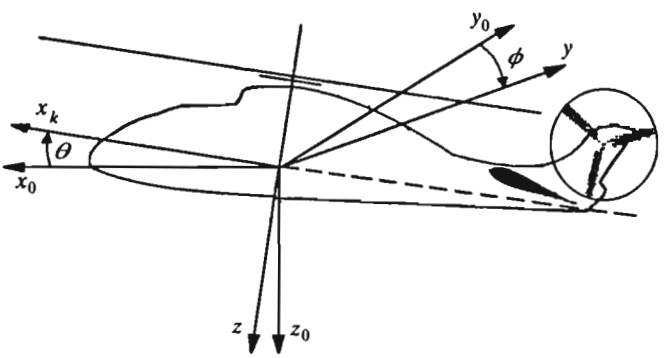

Fig. 4. Helicopter model

2.3. Forward flight

In the helicopter forward flight an induced velocity is a function of both the radial r and azimuth ψ coordinates, $\lambda_i = \lambda_i(r, \psi)$. Usually it is assumed, that the induced velocity distribution is linear along the blade and harmonic along the azimuth.

Most commonly applied is the Glauert model represented as

$$\lambda_i = \lambda_{io}[1 + \bar{x}(K_c \cos\psi + K_s \sin\psi)] \tag{2.13}$$

where only the first harmonic of azimuth is included.

In Glauert related models, the constant part λ_{io} of induced velocity in the forward flight is calculated as

$$\lambda_{io} = \sqrt{\frac{1}{2}\sqrt{\mu^4 + \frac{1}{4}C_T^2} - \mu^2} \tag{2.14}$$

Various values and formulae for calculating the coefficients K_c and K_s in Eq (2.13) are given in Table 3.

Table 3

mod. symb.	model formulae		refer.
F1	$K_c = 1.2$	$K_s = 0$	[7]
F2	$K_c = \tan(\chi/2)$	$K_s = 0$	[5]
F3	$K_c = (4/3)(1 - 1.8\mu^2)\tan(\chi/2)$	$K_s = -2\mu$	[6]
F4	$K_c = (4/3)\tan\chi/(1.2 + \tan\chi)$	$K_s = 0$	[13]
F5	$K_c = \sqrt{2}\sin\chi$	$K_s = 0$	[4]
F6	$K_c = (15\pi/32)\tan(\chi/2)$	$K_s = 0$	[13]
F7	$K_c = \sin^2\chi$	$K_s = 0$	[4]
F8	$K_c = (4/3)\frac{\mu}{\lambda}/(1.2 + \frac{\mu}{\lambda})$	$K_s = -(16e\mu^3)/(a\sigma_R t^4)$	[13]
F9	$K_c = 4C_{my}/C_T$	$K_s = 4C_{mx}/C_T$	[8]
MS	$\lambda_i = 4\lambda_{io}\left[(1/2)c_0 - \sum_{n=1}^{\infty} c_n(x, \alpha_w)\cos(n\psi)\right]$		[11,2]
DN	$\dot{\lambda}_i + (\mathbf{LM})^{-1}\lambda_i = \mathbf{M}^{-1}\mathbf{C}_{Fa}$ $\lambda_i = \lambda_m + \lambda_{i1} + \lambda_{i2}x\sin\psi + \lambda_{i3}x\cos\psi$		[14]

These coefficients are functions of μ and λ_i. The value of coefficient K_c is usually positive while the value of K_s is negative, so the value of induced velocity is greater at the rear part of rotor disk and at the side of rotor disk of retreating blade. The values originally suggested by Glauert (F1) were

$$K_c = 1.2 \qquad K_s = 0 \tag{2.15}$$

They were justified by analogy to elliptical distribution of the induced velocity *on a fixed wing.*

The skew of rotor wake was taken into account in other methods, given in Table 3.

In the method (F8) developed by Payne (1959), a taper of rotor blades is taken into account as an integral

$$t_4 = 4\int_0^{R_w} \frac{c(r)}{c(0)} r^3\, dr \tag{2.16}$$

The method (F9) of Johnson is a simplified version of the dynamic inflow model.

2.4. Influence of side velocity

In the formulae for forward flight it is assumed that the horizontal axis of induced velocity distribution coincides with a helicopter plane of symmetry.

When there is a side component V of the flight velocity, the inflow distribution should be rotated about the rotor vertical axis by the angle ϕ_0 from the fuselage plane of symmetry

$$\phi_0 = -\arcsin\frac{V}{\sqrt{U^2+V^2}} \tag{2.17}$$

and in Eq (2.13) the azimuth ψ should replaced by

$$\psi_k = \psi + \phi_0 \tag{2.18}$$

2.5. Ground effect

In a proximity of the ground, the effects of "air cushion" appears, which influences the values of induced velocity reducing the power needed to produce the required amount of thrust. The influence of ground proximity was investigated for instance by Zbrozek (1947).

Main factors influencing the value of induced velocity in the helicopter flight close to the ground are:

- Distance Z from the ground
- Value of the rotor thrust
- Vertical λ_c and horizontal μ components of the flight velocity.

The ground effect decreases with the increase in velocity μ of forward flight and for $\mu > 0.1$ disappears due to a large skew angle of the rotor wake (cf Johnson (1980)). The way of accounting for ground effects considered in this study (according to Cheeseman and Bennett (1955)), is given in Table 4.

Table 4

vertical flight	$\lambda_{ig}/\lambda_i = 1-(R/4Z)^2$
forward flight	$\lambda_{ig}/\lambda_i = 1-(R/4Z)^2[1+(\mu/\lambda)^2]^{-1}$

3. Helicopter model

The expressions of induced velocity described above are included into the computer model of a single rotor helicopter in a steady flight. This model

consists of fuselage, stabilisers, main and tail rotors. The equations of motion have been obtained considering equilibrium of forces and moments acting on helicopter components

$$\boldsymbol{F}_r + \boldsymbol{F}_t + \boldsymbol{F}_f + \boldsymbol{F}_s = \boldsymbol{0} \tag{3.1}$$

where $\boldsymbol{F}_f$, $\boldsymbol{F}_s$, $\boldsymbol{F}_r$, $\boldsymbol{F}_t$ represent the loads produced by: fuselage, stabilisers, main rotor and tail rotor, respectively.

The loads are calculated first in local systems of coordinates and then transformed to the helicopter system of coordinates. Six non-linear, coupled differential equations are obtained for flight state vector $\boldsymbol{X} = [U, V, W, P, Q, R]$.

3.1. Fuselage

The helicopter fuselage is modelled as a rigid body with six degrees of freedom. At the end of the tail boom there are a tail rotor and a horizontal stabiliser modelled as separate elements.

Fuselage loads result from aerodynamic, inertia, and gravity forces.

Calculations of the aerodynamic loads are based on the fuselage aerodynamic coefficients obtained from wind tunnel experiments. In this particular case the dependence of aerodynamic coefficients on the helicopter angular velocity and displacements is not taken into account. This does not seem to influence the results significantly, as stability is calculated in a steady flight for small disturbances. The angular velocities P, Q, R are included into calculation of the loads acting on a tail rotor and a stabiliser.

The influence of main rotor inflow on aerodynamic loads of the fuselage are accounted for as a contribution of the main rotor induced velocity to the total flow velocity taken into calculations of the fuselage angles of incidence and slip.

3.2. Stabilisers

In the helicopter computer model used in this study only the horizontal stabiliser is considered as vertical stabilisers are taken into account in fuselage aerodynamic loads. In this model the stabiliser angle of incidence can be varied. Aerodynamic loads are calculated from $2D$, steady flow with aerodynamic coefficients corrected for a low aspect ratio. The influence of rotor induced velocity is included in components of flow velocity taken for evaluation of the stabiliser angle of attack.

3.3. Main rotor

The main rotor is composed of b blades attached to the hub with coinciding a flap hinge and a pitch control bearing. The angular velocity Ω of the main rotor is constant, in a clockwise direction in a top view. The pitch control system is rigid. A precone angle, a spring (which represents the distributed stiffness of real blade) and a flap-pitch coupling due to kinematics of a real hub can be placed in the flap hinge.

All rotor blades are the same. The blades are rigid and twisted geometrically about the pitch axis. They can rotate freely in the flap hinge and are controlled by variation of a pitch angle. It is assumed that the angles of pitch control are defined as

$$\Theta = \Theta_0 + \Theta_1 \cos\psi + \Theta_2 \sin\psi \tag{3.2}$$

and flapping angles as

$$\beta = \beta_0 - \beta_1 \cos\psi - \beta_2 \sin\psi \tag{3.3}$$

The blade geometrical twist, hub precone angle and blade angle of rotation in the flap hinge are small and the blade equations of motion can be linearized.

Blade aerodynamic loads are calculated using two-dimensional steady, nonlinear airfoil characteristics. To calculate components of the flow velocity needed for calculating the blade angle of attack, different induced velocity models are included into analysis. In cross-sections of rotor blades, an aerodynamic centre is shifted from a pitch control axis. Blade aerodynamic loads are coupled with the rotor thrust and inflow velocity.

The blades steady motion described by flapping coefficients, Eq (3.3) is calculated by harmonic balance method.

The iteration algorithm used in calculation of rotor loads $\boldsymbol{F}_r$ is shown in Fig.5.

4. Tail rotor

The tail rotor rotates about the axis perpendicular to the helicopter plane of symmetry at constant angular velocity and advancing blade "down". Blades are identical and attached to the shaft with a flap hinge and a pitch bearing placed in the same point of the hub. The kinematic flap-pitch coupling is taken

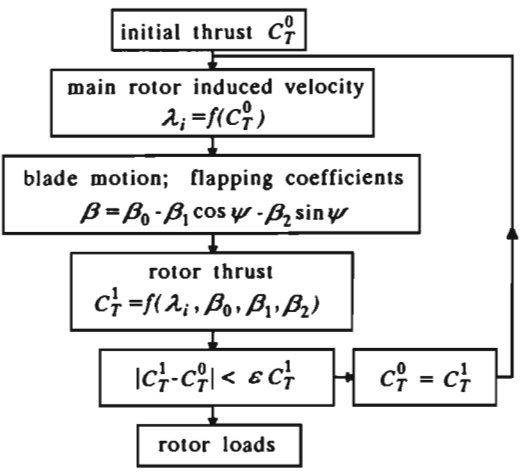

Fig. 5. Algorithm for calculation of main rotor loads

into account. The blades are rigid and geometrically twisted about pitch axis. Only collective pitch control Θ_{so} is applied.

A quasisteady, 2D model of aerodynamic loads is utilised with nonlinear aerofoil aerodynamic coefficients. The induced velocity is obtained from the Glauert model (F1). The contribution of the main rotor induced velocity is assumed as an increase in the flow velocity used for calculation of the angle of attack in a tail rotor blade section.

The first harmonic of steady blade flapping is calculated by harmonic balance method using the algorithm adjusting loads and inflow in a way similar to calculations of main rotor loads.

5. Steady flight conditions

In this study a helicopter in steady, forward flight is considered. The first part of stability analysis consists in calculation of flight conditions for which the helicopter stability is to be investigated. For given flight velocity, the vector of parameters of steady flight condition is defined as

$$\boldsymbol{S} = [\theta, \phi, \Theta_0, \Theta_1, \Theta_2, \Theta_{so}] \tag{5.1}$$

This vector is composed of: the helicopter pitch θ and roll ϕ angles and main rotor control angles of collective Θ_0 and cyclic Θ_1, Θ_2 pitch and tail rotor

collective pitch Θ_{so}. The state vector $\boldsymbol{S}$ is calculated from the system of six nonlinear algebraic equations describing equilibrium conditions of helicopter in steady flight. These equations are obtained from equations of motion by dropping the inertia loads and solved by the modified gradient method shown in Fig.6.

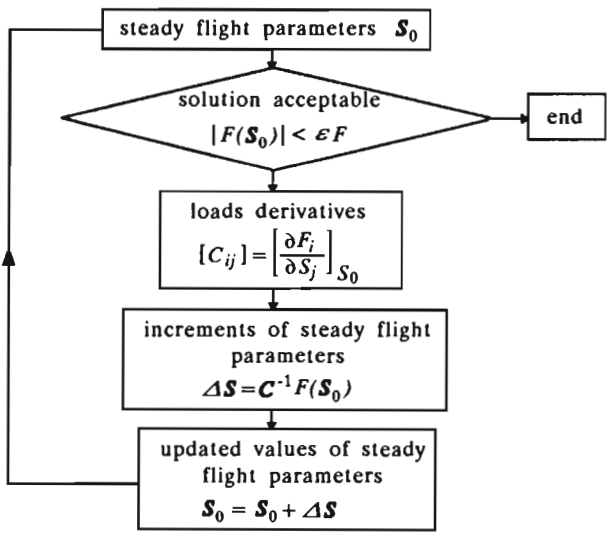

Fig. 6. Algorithm for computation of steady flight parameters

6. Stability analysis

For the stability analysis, the helicopter equations of motion are linearized using the steady flight conditions calculated above. This linearization is done by the finite difference method. The eigenvectors and eigenvalues of the state matrix are used for helicopter stability evaluation.

The algorithm for stability analysis is shown in Fig.7.

7. Results of computations

The objective of this study was to investigate the influence of main rotor

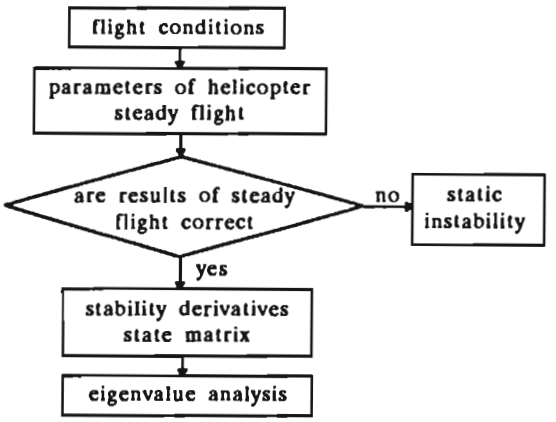

Fig. 7. Algorithm for helicopter stability investigation

induce velocity modelling on helicopter stability. The data used in computations concern the helicopter of total mass about 6 tons with the four blade main rotor, three blade tail rotor and horizontal stabiliser with the fixed angle of incidence.

The convergence limit in calculation of the rotor thrust for obtaining the main rotor flapping coefficients was 1% of its actual value. For computations of steady flight parameters, the convergence limit for iteration of forces was 500 N and 500 Nm for iteration of moments. State variables in calculation of stability derivatives were: 0.25 deg for angles, 0.25 m/s for linear velocity and 0.1 rad/s for angular velocity.

The flight cases covered by computations are given in Table 5.

Selected results of computations are presented in the next chapter.

Table 5

λ_c	μ	inflow model number
without ground effect		
0.0	$0.0 \div 0.35$	F1 ÷ F9, MS, DN
$-0.05 \div 0.03$	0.0	V1, V2, MS, DN
with ground effect $Z/R = 0.5 \div 2.0$		
0.0	0.05	F1 ÷ F9, MS, DN
−0.015	0.0	V1, V2, MS, DN

7.1. Vertical flight

For helicopter vertical flight a parameter of computation was the coefficient λ_c of vertical flight velocity within the range from -0.05 to 0.03. The results of calculations are plotted as functions of this parameter.

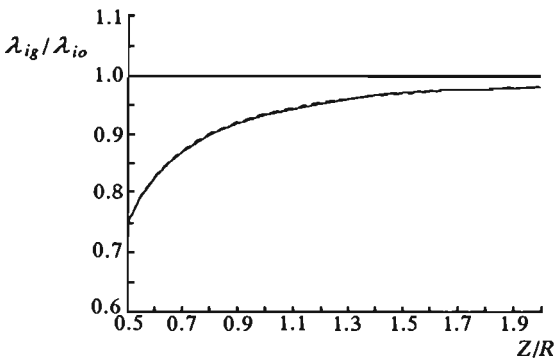

Fig. 8. Influence of a ground proximity on a mean value of induced velocity in helicopter hover

The influence of ground proximity on the mean value of induce velocity is presented in Fig.8. It was proved by computation, that parameters of steady flight as well as eigenvalues asymptotically approach the values in free flight, as the distance from the ground increases.

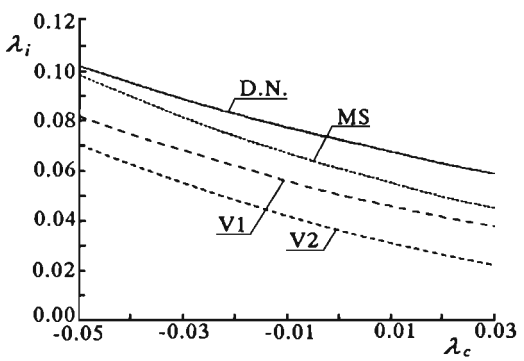

Fig. 9. Mean induced velocity in helicopter vertical climb calculated for different inflow models

In Fig.9 the induced velocities calculated for all axial flow models are presented. An induced velocity depends on a flight velocity in a similar way

for all the inflow models considered.

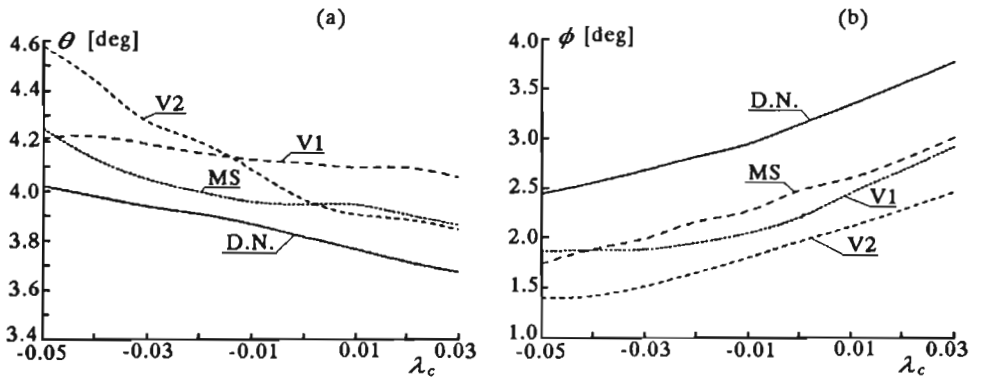

Fig. 10. Pitch and roll angles of a helicopter in vertical climb for different inflow models

The same trend can also be observed for the helicopter pitch θ and roll ϕ angles shown in Fig.10; there is no significant change in a shape of curves due to variations of the inflow model.

Constant blade flapping β_0 and collective pitch Θ_0 angles of the main rotor (not shown here) depend in the same way on the model of induced velocity. In this case the cyclic flapping and pitch control appeared in axial flight, which can be attributed to non-zero roll and pitch angles of the helicopter. The variation in harmonics of flap and pitch angles depends on the model and is more intensive for Θ_2 and β_2.

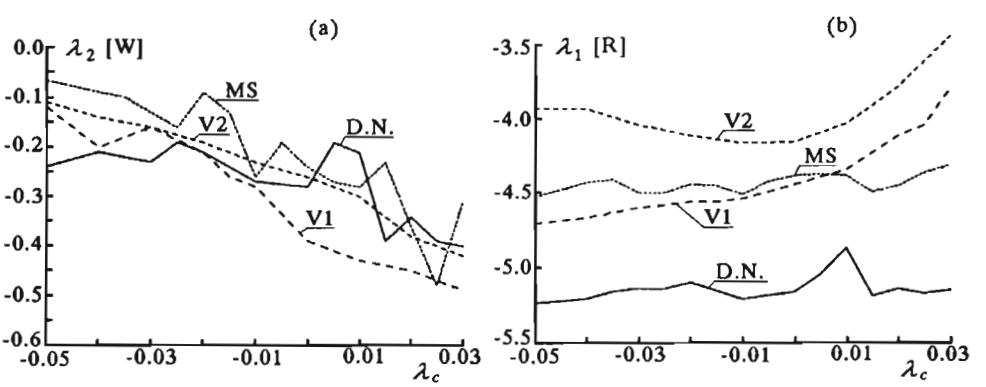

Fig. 11. Eigenvalues corresponding to helicopter vertial velocity and yaw angle for climbing as function of inflow models

The sample results of stability investigation for axial flight are shown in Fig.11. The eigenvalues related to the yaw velocity, horizontal and vertical translation have only real parts. The shape of $\lambda_w(\lambda_c)$ curve (Fig.11a) is irregular probably due to accuracy of numerical calculations.

The most important differences resulting from the application of different induced velocity models appear mainly in the yaw motion (Fig.11.b) and unsteady lateral (not shown here) motion. But no phenomena are observed, such as changing rapidly the character of the motion or transferring the stable motion into unstable one due to variation of inflow model. The effects of changing the induced velocity model are only quantitative not qualitative.

7.2. Forward flight

The analysis of forward flight case covers investigation of the influence of:

- Glauert type models
- Models of different type
- Proximity of the ground.

In the forward flight case the parameter of computations was the helicopter advance ratio μ.

During the computations, it was revealed that the Glauert-type models give similar results for the helicopter pitch angle θ, tail rotor pitch angle Θ_{so}, and constant coefficients of induced flow λ_{io}. In the constant part of flapping β_0 and collective pitch Θ_0 the shift of vales can be observed, but without changes in the shape of curves. The obvious differences appear between the values of cyclic components λ_{i1}, λ_{i2} of the inflow, but surprisingly they affect mainly the control of the main rotor and helicopter roll angle ϕ. The stability results are not changed by variation of cyclic components of the induced velocity instead of unsteady longitudinal motion.

The influence of models of different type on steady flight parameters is presented in Fig.12. Changing of model affects mainly the helicopter trimmed roll angle ϕ, periodic components of the rotor control and collective pitch of the tail rotor. There is almost no influence of inflow model on the rotor motion.

For some eigenvalues the results of stability analysis is not inflicted by changing a model, but the influence on some eigenvalues is significant (Fig.13a,b).

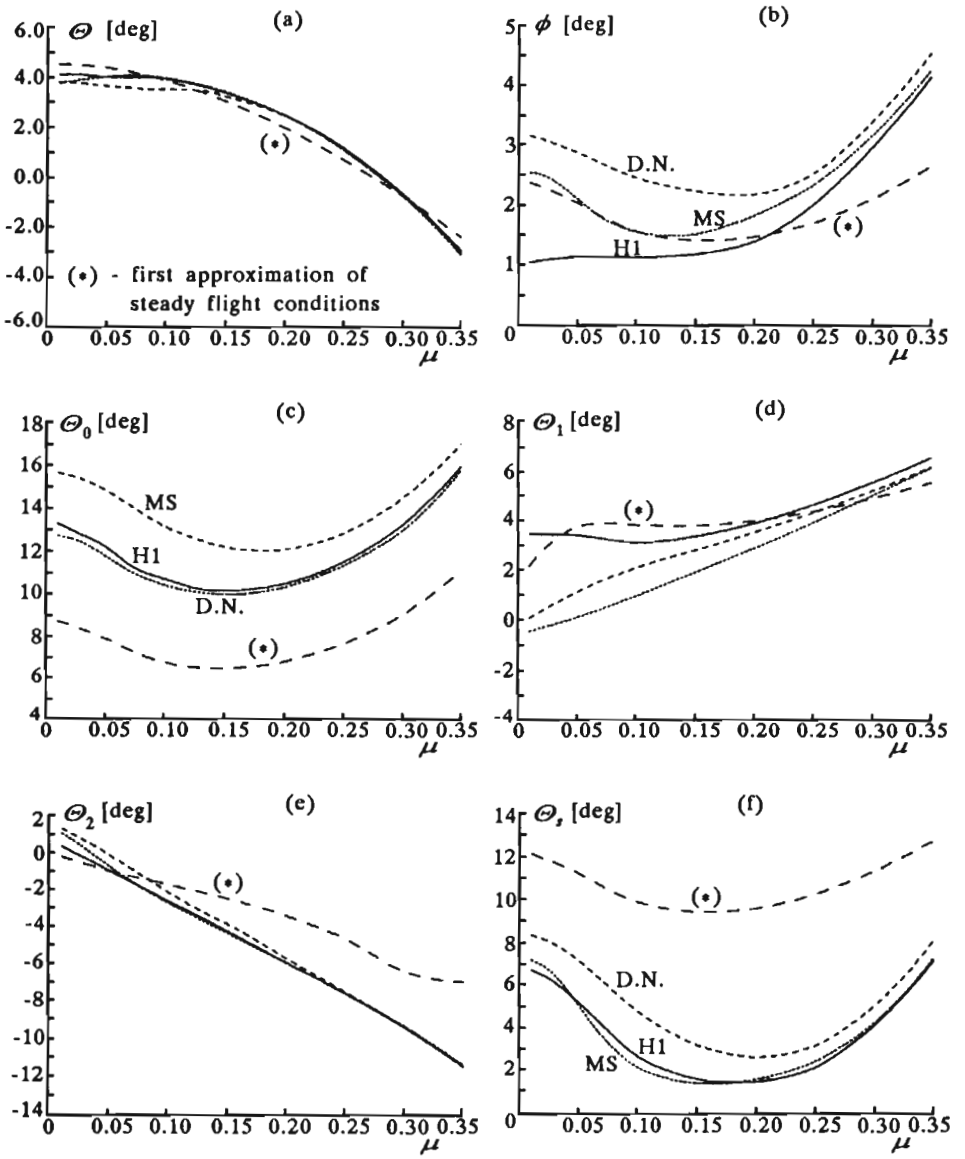

Fig. 12. Helicopter trim angles in forward flight for different inflow models

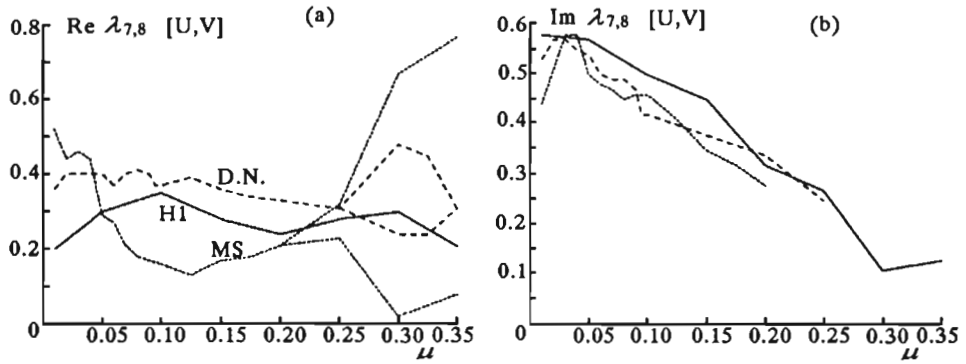

Fig. 13. Eigenvalue correspnding to helicopter horizontal velocity in forward flight

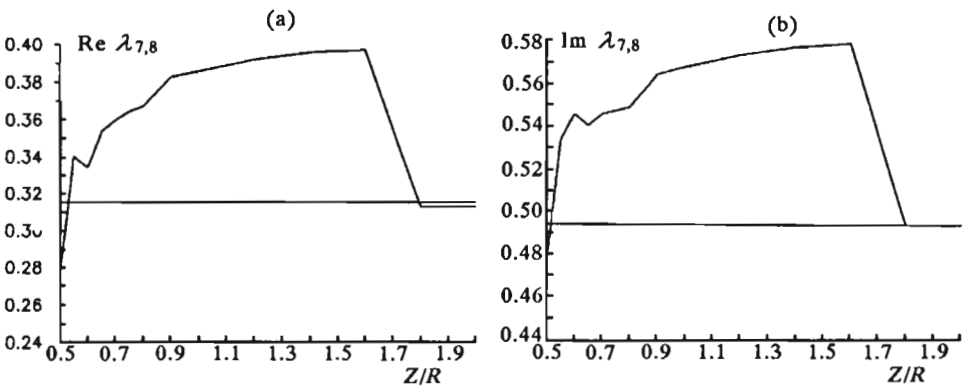

Fig. 14. An example of eigenvalue variation in forward flight for Mangler-Square inflow model as function of rotor distance from the ground

The influence of proximity of the ground is shown in Fig.14 for the Mangler & Squire model. Approaching to ground, the character of helicopter disturbed motion is changed and flight stability can be deteriorated.

8. Conclusions

Different induced velocity models of the helicopter main rotor were included into calculation of trim and stability parameters of helicopter steady flight. Two specialised models in hover, nine Glauert-type models in forward flight,

dynamic inflow and the Mangler & Squire models for vertical and forward flight, with and without ground effect were analysed.

In vertical flight the results of calculations revealed dependence of calculated parameters on the inflow modelling for all the velocities considered. Due to roll and pitch angles needed to trim the helicopter, harmonic components of flapping and cyclic control appeared in axial flight.

In forward flight the Glauert-type models give similar results for steady flight parameters and stability results.

Models of different type differentiate results of stability calculations, but have no influence on the blade motion.

As a general conclusion from this study it can be stated, that the induced velocity models usually considered do not change the character of helicopter motion; i.e., do not destabilise or alter significantly the trim parameters.

The proximity of the ground affects both steady flight parameters and stability, but its influence is decreasing when the distance of the rotor from the ground increases.

To chose the best model for practical calculations, flight tests should be performed.

References

1. *British Civil Airworthiness Requirements – Part G – Helicopters*
2. BRAMWELL A.R.S., 1976, *Helicopter Dynamics,* Edward Arnold Ltd
3. CHEESEMAN I.C., BENNETT W.E., 1995, The Effect of the Ground on a Helicopter Rotor in Forward Flight, *A.R.C. R&M,* 3021
4. CHEN R.T.N., 1989, A Survey of Nonuniform Inflow Models for Rotorcraft Flight Dynamics and Control Applications, *XV European Rotorcraft Forum,* Paper 64, Amsterdam
5. COLEMAN R.P., FEINGOLD A.M., STEMPIN C.W., 1945, Evaluation of the Inducted Velocity Field of an Idealised Helicopter Rotor, *NASA ARR L5E10*
6. DREES J.M.JR., 1949, A Theory of Airflow Trough Rotors and its Application to Some Helicopter Problems, *Journal of Helicopter Association of Great Britain,* **3**, 2
7. GESSOW A., MYERS G.C.JR., 1985, *Aerodynamics of the Helicopter,* Frederick Ungar Pub. Co., New York
8. JOHNSON W., 1980, *Helicopter Theory,* Princeton Univ. Press
9. KOWALECZKO G., 1991, An Analysis of Spatial Helicopter Motion Including the Influence of Autopilot, Ph.D. Thesis (in Polish), WAT, Warszawa

10. ŁUCJANEK W., NARKIEWICZ J., SIBILSKI K.. 1986, Dynamic Stability of Helicopter with Articulated Rotor, *Journal of Theoretical and Applied Mechanics*, **24**, 1-2

11. MANGLER K.W., SQUIRE H.B., 1950, The Inducted Velocity Field of a Rotor, *A.R.C., R&M*, 2642

12. NARKIEWICZ J., SYRYCZYŃSKI J., 1992, Calculation of Unsteady Aerodynamic Aerofoil Loads in State Variables, (in Polish), *Mechanika w Lotnictwie*, PTMTiS

13. PAYNE P.R., 1959, *Helicopter Dynamics and Aerodynamics*, Sir Isaac Pitman & Sons, LTD, London

14. PETERS D.A., HAQUANG N., 1988, Dynamic Inflow for Practical Application, *Journal of the American Helicopter Society*, **33**, 4

15. ZBROZEK F., 1947, Ground Effect on the Lifting Rotor, *R.A.E.*, 2347

Wpływ modelowania prędkości indukowanej na stateczność śmigłowca

Streszczenie

Dla różnych stanów lotu: zawis, lot pionowy i poziomy z i bez wplywu ziemi zbadano wplyw modelowania rozkladu prędkości indukowanej wirnika nośnego na stateczność śmigłowca.

W pracy dokonano przeglądu zależności opisujących rozkłady prędkości indukowanej wirnika i oceniono ich przydatność w zastosowaniu do badania stateczności. Wybrane modele wykorzystano do obliczenia parametrów lotu ustalonego, prawych stron zlinearyzowanych równań ruchu oraz wartości i wektorów własnych macierzy stanu.

Badanie stateczności śmigłowca w locie ustalonym pokazało, że różnice wyników otrzymane dla różnych zależności typu Glauerta opisujących prędkość indukowaną jako rozkład harmoniczny wzdłuż azymutu i liniowy wzdłuż długości są niewielkie.

Inne modele prędkości indukowanej jak: Manglera-Squire'a i dynamicznego napływu nie zmieniają charakteru ruchu śmigłowca, ale ilościowo wpływają na wyniki badania stateczności.

Manuscript received October 28, 1994; accepted for print February 7, 1995